Testing excitation models of rapidly oscillating Ap stars with interferometry

M. S. Cunha, D. Alentiev, I. M. Brandão, K. Perraut

Monthly Notices
of the
ROYAL ASTRONOMICAL SOCIETY

MNRAS **436,** 1639–1647 (2013) doi:10.1093/mnras/stt1679
Advance Access publication 2013 October 1

Testing excitation models of rapidly oscillating Ap stars with interferometry

M. S. Cunha,[1,2]★ D. Alentiev,[3] I. M. Brandão[1] and K. Perraut[4]

[1]*Centro de Astrofísica da Universidade do Porto, Rua das Estrelas, P-4150-762 Porto, Portugal*
[2]*Sydney Institute for Astronomy (SIfA), School of Physics, University of Sydney, NSW 2006, Australia*
[3]*Department of Physics, Tavrian National University, Vernadskiy's Avenue 4, UA-95007 Simferopol, Ukraine*
[4]*UJF-Grenoble 1/CNRS-INSU, Institut de Planétologie et d'Astrophysique de Grenoble (IPAG) UMR 5274, Grenoble, F-38041, France*

Accepted 2013 September 4. Received 2013 September 3; in original form 2013 June 13

ABSTRACT

Rapidly oscillating Ap stars are unique objects in the potential they offer to study the interplay between a number of important physical phenomena, in particular, pulsations, magnetic fields, diffusion and convection. Nevertheless, the simple understanding of how the observed pulsations are excited in these stars is still in progress. In this work, we perform a test to what is possibly the most widely accepted excitation theory for this class of stellar pulsators. The test is based on the study of a subset of members of this class for which stringent data on the fundamental parameters are available thanks to interferometry. For three out of the four stars considered in this study, we find that linear, non-adiabatic models with envelope convection suppressed around the magnetic poles can reproduce well the frequency region where oscillations are observed. For the fourth star in our sample no agreement is found, indicating that a new excitation mechanism must be considered. For the three stars whose observed frequencies can be explained by the excitation models under discussion, we derive the minimum angular extent of the region where convection must be suppressed. Finally, we find that the frequency regions where modes are expected to be excited in these models are very sensitive to the stellar radius. This opens the interesting possibility of determining this quantity and related ones, such as the effective temperature or luminosity, from comparison between model predictions and observations, in other targets for which these parameters are not well determined.

Key words: stars: chemically peculiar – stars: evolution – stars: individual: HD 201601 – stars: individual: HD 176232 – stars: individual: HD 137909 – stars: individual: HD 128898.

1 INTRODUCTION

Rapidly oscillating Ap (roAp) stars are chemically peculiar stars which pulsate in modes of high radial order (Kurtz 1982) and are found among the coolest subgroup of Ap stars, usually showing abundance anomalies in lines of ions of Sr, Cr, rare earth elements and in the core of the hydrogen line. In addition to specific chemical peculiarities, these cool Ap stars are characterized by their slow rotation, with periods that range between days and many decades, and strong magnetic fields, with typical intensities of a few kG, but which in some stars can reach values higher than 20 kG (e.g. Hubrig et al. 2005).

Presently, there are about 45 roAp stars known with oscillation periods varying between a little more than 20 min (Elkin et al. 2005; Alentiev et al. 2012) and a little less than 6 min (Kreidl & Kurtz 1986; Saio et al. 2012). There is some observational indication that the roAp stars with long pulsation periods are relatively evolved, i.e. they are approaching the terminal-age main sequence. However, the distribution of roAp stars in the HR diagram and, hence, their evolutionary status is hard to establish due to the difficulty in determining their effective temperatures, which, in turn, results from the surface chemical peculiarities and the associated horizontal and vertical abundance gradients. To complicate matters further, accurate parallaxes are available only for about one third of the known roAp stars. Despite this, the data available so far are enough to establish that roAp stars are positioned in the main-sequence part of the classical instability strip, having effective temperatures between about 6400 and 8100 K and luminosities between $\log(L/L_{\odot}) \sim 0.8$ and ~ 1.5 (see, e.g., Kochukhov 2009 and Cunha 2007 for observational and theoretical reviews on roAp stars).

The mechanism responsible for the excitation of the oscillations observed in roAp stars is not yet fully understood. Over the years there have been a number of suggestions regarding this mechanism, ranging from the direct effect of the Lorentz force to magnetic overstability and the opacity mechanism (see Cunha 2002, and

★ E-mail: mcunha@astro.up.pt

references therein). Nevertheless, only in a few cases non-adiabatic calculations leading to the computation of mode growth rates were performed to investigate on mode stability.

Unstable, high radial order modes, similar to those observed in roAp stars, were found in the models presented by Gautschy, Saio & Harzenmoser (1998), Balmforth et al. (2001), Saio (2005) and Théado et al. (2009). These models differ substantially in their physical assumptions. Gautschy et al. (1998) considered that roAp stars may have a chromosphere and made an ad hoc modification to a temperature–optical depth relation such as to induce a temperature inversion at small optical depths. Balmforth et al. (2001) considered that the strong magnetic field present in roAp stars suppresses envelope convection in some region around the magnetic poles and, thus, built a spotted model in which only the magnetic equatorial region retains envelope convection. In addition, they considered models including the presence of a polar wind. Saio (2005) considered models in which envelope convection is fully suppressed and in which the direct effect of the magnetic field on the oscillations is taken into account. Finally, Théado et al. (2009) considered both models with and without envelope convection suppressed and different metallicity abundances and metallicity profiles. Despite differences in the physical assumptions, in all of these models the excitation of the high radial order oscillations found as a result of the non-adiabatic computations originates from the opacity mechanism acting in the hydrogen ionization region.

Even though the computations described above predict the excitation of high radial order pulsations, not all observed pulsation properties of roAp stars are well reproduced by these models. In particular, models do not seem to predict the instability of the very high frequencies, well above the standard acoustic cutoff, observed in some roAp stars. In addition, difficulties were found in reproducing the observed red edge of the instability strip (Cunha 2002; Théado et al. 2009).

The range of frequencies excited by the opacity mechanism depends strongly on the star's effective temperature and luminosity. Thus, the comparison between model predictions and observations requires the accurate determination of these quantities. With the recent development of interferometers (see Cunha et al. 2007 for a review), the determination of effective temperatures only weakly dependent on atmospheric models became possible for a few roAp stars. In this paper, we will use these interferometrically based effective temperature determinations, along with the stars' luminosities derived from the combination of *Hipparcos* parallaxes and the stars' bolometric fluxes, to test the models proposed by Balmforth et al. (2001). In Section 2, we will briefly describe the models and the observables for the four roAp stars that have measured angular diameters. In Section 3, we will present the results of the model computations for the four stars and in Section 4, we will discuss the results and conclude.

2 MODELS AND OBSERVABLES

2.1 Observables

The angular diameters of four roAp stars, namely α Cir (Bruntt et al. 2008), β CrB (Bruntt et al. 2010), 10 Aql (Perraut et al. 2013) and γ Equ (Perraut et al. 2011), have recently been determined using the Sydney University Stellar Interferometer, in the first case, and the CHARA interferometric array, in the latter three cases. Moreover, bolometric fluxes were also calculated for these stars, based on calibrated spectra. These angular diameters were then used, in combination with the bolometric fluxes, to derive the stars' effective temperatures in a way that is less dependent on the modelling of the complex atmospheric structure of these stars, than other traditional approaches, such as those based on the analysis of photometric or spectroscopic data. Moreover, *Hipparcos* parallaxes were combined with the bolometric fluxes to derive the stars' luminosities.

The effective temperatures and luminosities found in the works mentioned above will be used as input for the models presented here. For the remaining of this paper, we shall refer to these inputs as the *interferometric inputs*. These are listed in Table 1 together with photometric and spectroscopic temperature determinations published in the literature for the same stars. Amongst the classical methods used to determine effective temperatures, those based on high-resolution spectroscopy are commonly thought to yield the most reliable results for chemically peculiar stars. Advanced atmospheric models, based on the LLMODELS code (Shulyak et al. 2004), which include individual abundances and an empirical chemical stratification of elements, have recently been used to derive fundamental parameters of a number of roAp stars, including those under

Table 1. Effective temperatures and luminosities for the four test stars considered in this work.

Star		Interferometric inputs		Spectroscopic inputs		Photometric inputs	
HD	Other	[a]$T_{\rm eff}$ (K)	[a]$L/{\rm L}_{\odot}$	[b]$T_{\rm eff}$ (K)	[b]$L/{\rm L}_{\odot}$	[c]$T_{\rm eff}$ (K)	[c]$L/{\rm L}_{\odot}$
201601	γ Equ	[d]7364 ± 235	12.8 ± 1.4	7550 ± 50	12.6 ± 0.9	7621 ± 200	12.6 ± 0.9
176232	10 Aql	[e]7900 ± 200	[e]18.5 ± 1.6	7550 ± 50	[f]18.7 ± 0.9	7925 ± 200	20.9 ± 2.0
137909	β CrB	7980 ± 180	25.3 ± 2.9	8100 ± 50	23.7 ± 1.9	7430 ± 200	27.5 ± 1.3
128898	α Cir	7420 ± 170	10.5 ± 0.6	7500 ± 130	10.7 ± 0.3	7673 ± 200	11.0 ± 0.3

Notes. [a]$T_{\rm eff}$ values derived based on interferometry and L values derived based on *Hipparcos* parallax and bolometric flux (Bruntt et al. 2008, 2010; Perraut et al. 2011, Perraut et al. 2013). [b]$T_{\rm eff}$ and L values derived from advanced atmospheric models and high-resolution spectroscopy (Kochukhov, Shulyak & Ryabchikova 2009; Nesvacil et al. 2013; Shulyak, Ryabchikova & Kochukhov 2013). [c]$T_{\rm eff}$ values derived based on Geneva photometric indices and L values derived based on *Hipparcos* parallax using standard bolometric corrections (Kochukhov & Bagnulo 2006).

[d]This value may be in excess by up to 110 K due to the presence of a close companion (see Perraut et al. 2011 for details).

[e]This value corresponds to the average of the two values given in Perraut et al. (2013).

[f]The luminosity value adopted here is the average of the two values presented for He-normal atmospheric models in the work by Nesvacil et al. (2013), for an effective temperature of 7550 K and model calibrations based on space or ground-based data, respectively.

Table 2. Observed frequency range of the pulsations exhibited by the four test stars considered in this work.

HD	Other	Frequency range (mHz)
201601	γ Equ	[a]1.31–1.42
176232	10 Aql	[b]1.39–1.45
137909	β CrB	[c]1.03
128898	α Cir	[d]2.26–2.57

Notes. [a]From Gruberbauer et al. (2008). [b]From Huber et al. (2008). [c]From Kurtz et al. (2007) (single frequency). [d]From Bruntt et al. (2009).

consideration here. We shall refer to these as the *spectroscopic inputs*. Inspection of Table 1 shows that for three out of the four stars in our sample, the effective temperatures derived from these models are in reasonable agreement with the values derived from interferometry. For comparison, we consider also the effective temperatures determined by Kochukhov & Bagnulo (2006) based on photometric data. Our choice for the latter, over other photometric temperature determinations published in the literature, is based on the fact that the above-mentioned authors computed effective temperatures for the four stars under consideration through exactly the same procedure. Hence, this set of photometric values may be considered, as much as possible, as an homogenous set. For the remaining of the paper, we shall refer to the values of $T_{\rm eff}$ and L derived by Kochukhov & Bagnulo (2006) as the *photometric inputs*.

In addition to the effective temperatures and luminosities, the test of the proposed non-adiabatic computations requires knowledge of the pulsation properties of the roAp stars, in particular of the characteristic frequencies of the observed modes. These are presented in Table 2, for the four stars under consideration. For this work, the actual values of the individual frequencies are not of importance. Only the range of observed frequencies in each star needs to be considered, as an indicator of the frequency region in which modes are excited. We note, however, that recent observations of roAp stars by the NASA *Kepler* satellite (Balona et al. 2011a,b; Kurtz et al. 2011), as well as the earlier debate about the roAp nature of β CrB (Hatzes & Mkrtichian 2004; Kurtz, Elkin & Mathys 2007), show that the amplitudes of the oscillations in roAp stars may in many cases be below observational detection. Moreover, it is clear from the *Kepler* data that the amplitudes of the modes observed in a single roAp star can differ by as much as one order of magnitude. Thus, for the purpose of testing theoretical models, each frequency range given in Table 2 should be taken as the smallest range possible, i.e. to be in agreement with the observations, theoretical models should predict mode excitation in the given frequency range, but not necessarily only within that frequency range.

2.2 Models and key parameters

To perform linear, non-adiabatic calculations for the four test stars considered in this work, we followed the approach presented by Balmforth et al. (2001). A detailed description of the corresponding models and physical assumptions can be found in the latter. Here, we briefly summarize those aspects that are important for the present discussion. The computations are based on two programs. The first generates an equilibrium envelope model, which does not include the energy generation core of the star and the second solves the linearized non-adiabatic pulsation equations for radial oscillations. The model considers that the strong magnetic field present in roAp stars is capable of suppressing envelope convection at least in some region around the magnetic poles. Two options are possible regarding the suppression of convection. The first suppresses envelope convection at all latitudes, producing a spherically symmetric equilibrium model. The second simulates a model in which convection is suppressed only up to some colatitude measured from the magnetic poles. In the latter case, two spherically symmetric equilibrium models are computed, one with envelope convection suppressed, hereafter *the polar model*, and the other with normal convection, treated with a non-local mixing length prescription described by Gough (1977), hereafter *the equatorial model*. The two equilibrium models are then matched such as to guarantee that they have the same internal structure. That is done by adjusting the luminosity and radius of one of the models until the same temperature, pressure and helium abundance is obtained in the two models below the convective envelope. As a result of the matching of the interior, the outer layers of the two equilibrium models will differ and so will their radii and luminosities. However, as discussed in Balmforth et al. (2001), the difference in luminosity between the two models will generally be smaller than that induced by line blanketing in a typical Ap star. As a consequence, it is not possible to derive the extent of the angular region around the magnetic pole in which envelope convection is suppressed directly from observations of the stellar surface.

When envelope convection is not suppressed at all latitudes, linear non-adiabatic radial eigenfrequencies are computed separately for each of the two spherically symmetric equilibrium models. Moreover, the linearized non-adiabatic equations in the equatorial model are solved using a non-local, time-dependent treatment of convection (Balmforth 1992, and references therein). The eigenfrequencies of the two spherically symmetric models are then used to compute the eigenfrequencies of the composite model (i.e. the model composed of the polar and equatorial regions), through the application of the variational principle.

Clearly, the procedure described above is oversimplified in a number of ways, as it neglects the direct effects of the Lorentz force on the equilibrium structure as well as on the pulsations. In addition, it presumes that like in the case of convective motions, the complex dynamics that would arise in the outer layers as a consequence of the horizontal hydrostatic unbalance is prevented by the action of the magnetic field. Producing a realistic model for these spotted stars would require a much higher degree of sophistication, which is beyond the scope of this paper. Instead, our aim is to test the model as presented by Balmforth et al. (2001), which has so far been quite successful in explaining the observations against the best data currently available.

In addition to defining the extent of the angular region around the magnetic pole in which envelope convection is to be suppressed and fixing the parameters associated with the treatment of convection, the proposed non-adiabatic calculations require the following relevant information.

(1) The minimum optical depth in the equilibrium model, $\tau_{\rm min}$. In the atmosphere, the thermal stratification is derived from a temperature–optical depth ($T-\tau$) relation fitted to a model atmosphere of Kurucz (Shibahashi & Saio 1985). The value of $\tau_{\rm min}$ is a free parameter of the model. For oscillations with frequencies well below the acoustic cutoff, the form of the eigenfunctions in the propagation cavity should be relatively independent of the value of $\tau_{\rm min}$ adopted. Nevertheless, in the case of the high-frequency oscillations observed in roAp stars, the form of the eigenfunctions below

Table 3. Model parameters of non-adiabatic calculations. Shown are two star identifications, model mass and model radius, as derived from the interferometric, spectroscopic and photometric inputs, respectively, interior hydrogen and helium abundances, surface helium abundance, minimum optical depth and outer boundary condition in the pulsation code. For the latter three entries two options have been used. The standard model uses the options shown in roman font, while other models are built by swapping to the italic font entries, one at the time.

HD	Other	Mass ($M_\odot$)	[a]$R_{\rm int}$ ($R_\odot$)	$R_{\rm spe}$ ($R_\odot$)	$R_{\rm pho}$ ($R_\odot$)	$X_{\rm int}$	$Y_{\rm int}$	$Y_{\rm sur}$	$\tau_{\rm min}$	BC
201601	γ Equ	1.75	2.20	2.08	2.04	0.705	0.278	0.01–*0.1*	3.5×10^{-5}–*3.5* $\times$ *10*$^{-4}$	reflect.–*transm.*
176232	10 Aql	1.95	2.31	2.53	2.43	0.705	0.278	0.01–*0.1*	3.5×10^{-5}–*3.5* $\times$ *10*$^{-4}$	reflect.–*transm.*
137909	β CrB	2.05	2.64	2.48	2.67	0.705	0.278	0.01–*0.1*	3.5×10^{-5}–*3.5* $\times$ *10*$^{-4}$	reflect.–*transm.*
128898	α Cir	1.70	1.96	1.94	1.88	0.705	0.278	0.01–*0.1*	3.5×10^{-5}–*3.5* $\times$ *10*$^{-4}$	reflect.–*transm.*

Notes. [a]The actual inputs to the code are the effective temperature and luminosity. These radii are derived from those inputs, and due to approximations in the last digits of $T_{\rm eff}$ and L they may differ from the published interferometric radii in the last decimal place.

the photosphere is more sensitive to the details of the overlaying atmosphere. With this in mind, we consider two different values of $\tau_{\rm min}$ in our computations, namely $\tau_{\rm min} = 3.5 \times 10^{-5}$ and 3.5×10^{-4}, in order to inspect the effect of changing this parameter on the results.

(2) The helium profile in the equilibrium model. The helium profile in models with envelope convection suppressed is determined according to the prescription presented in Balmforth et al. (2001), without a polar wind (so, with the accumulation parameter, A, set to zero). The profile is then characterized by a single parameter, $Y_{\rm surf}$, that establishes the helium at the surface. In our calculations, we assume that helium settles efficiently when convection is suppressed, leading to a very small helium abundance throughout the outermost layers, in particular where the hydrogen ionization takes place. When envelope convection is maintained, we assume a homogeneous helium profile. These assumptions are supported by the results of the work by Théado, Vauclair & Cunha (2005). To see the impact of the settling efficiency on the results, we consider two cases, corresponding to $Y_{\rm surf} = 0.1$ and 0.01.

(3) The outer mechanical boundary condition to be applied at the temperature minimum in the pulsation model. In some roAp stars, the frequencies of the observed oscillations are greater than the acoustic cutoff frequency, i.e. the frequency above which acoustic waves will propagate away into the atmosphere of the star and dissipate. This fact has been discussed in the literature at length. In particular, Sousa & Cunha (2008) suggested that the coupling of the oscillations with the magnetic field in the outer layers of roAp stars results in part of the original acoustic wave energy being converted into magnetic wave energy. The authors argue that the magnetic part of the energy is not dissipated, allowing a fraction of the wave energy to be retained in each pulsation cycle. In the non-adiabatic calculations considered here, the direct effect of the magnetic field on the oscillations, and thus its effect of the reflection of the modes, is not taken into account. Hence, the natural boundary condition to apply at the outer boundary is one that allows the wave to propagate away if its frequency is above the acoustic cutoff. That boundary condition is one of the possible options of the pulsation code used in this work and is derived from the matching of the solutions to a plane-parallel isothermal atmosphere. We shall call it the *transmissive boundary condition*. Despite the above, it is clear from the observations that a mechanism for the reflection of the highest frequency modes is missing in this non-magnetic model. In an attempt to account for the effect of such physical mechanism, Balmforth et al. (2001) considered a second option for the outer boundary condition which fully reflects the waves. We shall call it the *reflective boundary condition*. The latter corresponds to the low-frequency limit of the boundary condition obtained when matching the solutions on to an infinite isothermal atmosphere. Similarly, in this work, we consider the two alternative outer boundary conditions described in detail in Balmforth et al. (2001).

A summary of the properties of the models used for the present study is presented in Table 3. Our default set of models are calculated with $\tau_{\rm min} = 3.5 \times 10^{-5}$, $Y_{\rm surf} = 0.01$ and the reflective boundary condition. Also, all our models were computed assuming interior chemical abundances of helium and hydrogen of, respectively, $Y_{\rm int} = 0.278$ and $X = 0.705$ [similar to the solar helium and hydrogen abundances derived from Serenelli & Basu (2010) and Grevesse & Noels (1993)]. We note that we have considered the impact of adopting, instead, an interior chemical composition similar to that proposed by Asplund et al. (2009) for the bulk of the sun and found that the impact on the results was negligible, when compared with the other effects under study. For the stellar mass, we assumed $M = 1.75\ M_\odot$ for γ Equ, $M = 1.95\ M_\odot$ for 10 Aql, $M = 2.05\ M_\odot$ for β CrB and $M = 1.70\ M_\odot$ for α Cir. These values are within $\pm 0.05\ M_\odot$ of the values derived based on stellar evolution, given the spectroscopic input parameters considered in Table 1 and the above-mentioned envelope chemical abundances. They are also very close to the values derived by Kochukhov & Bagnulo (2006) for the same stars based on the photometric inputs.

3 RESULTS

Figs 1–3 summarize the results of the non-adiabatic calculations obtained for the stars in our sample. In the calculations, the oscillations are assumed to have a time dependence of the type $e^{-i\omega t}$, where the angular frequency $\omega = \omega_r + i\,\eta$. Thus, the oscillations are intrinsically unstable if the growth rates, η, are greater than zero.

3.1 Equatorial models

The growth rates obtained for equatorial models of the four stars in our sample are shown in Fig. 1. For each star, results are shown for three different models, including the default model and otherwise similar models but with a different value of the minimum optical depth or with a different outer boundary condition in the pulsation code. The radial orders of the modes shown are such as to encompass the region of observed frequencies. These are, respectively, $n = 10$–36 in the case of γ Equ, 10 Aql and β Crb, and $n = 19$–39 in the case of α Cir.

In all cases, and for all four stars, modes in the frequency region where oscillations are observed were found to be intrinsically stable in the equatorial models. From inspection of the gas pressure and turbulent pressure contributions to the growth rates, obtained from the computation of the cumulative work integrals (see Balmforth et al. 2001 for details), we found that in all these models the turbulent

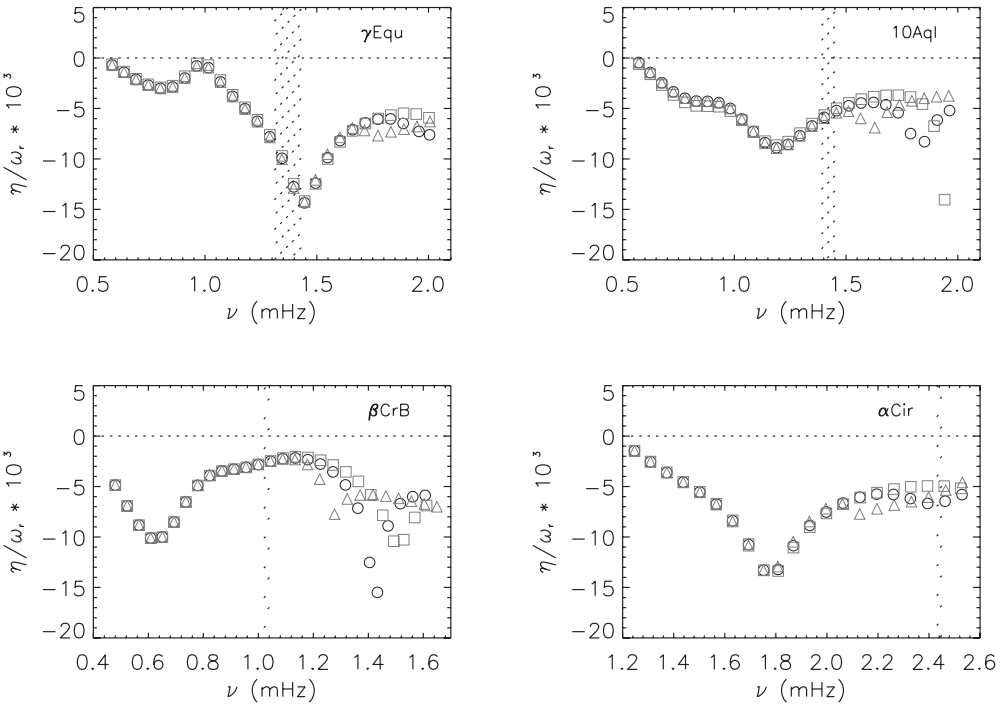

Figure 1. Normalized growth rates for equatorial regions (i.e. without suppression of convection) as function of the cyclic frequency $\nu = \omega/2\pi$. The modes are unstable when the normalized growth rates are greater than zero. The results are shown for the interferometric inputs of: γ Equ (top, left), 10 Aql (top, right), β CrB (bottom, left) and α Cir (bottom, right). For each star, we show results for the default case (circles), for the case with $\tau_{\rm min} = 3.5 \times 10^{-4}$ (squares) and for the case with transmissive boundary condition (upward triangles). All equatorial models have homogeneous chemical composition in the envelope. In each panel, zero growth rate is indicated by the horizontal dashed line and the shadowed region marks the range of observed frequencies.

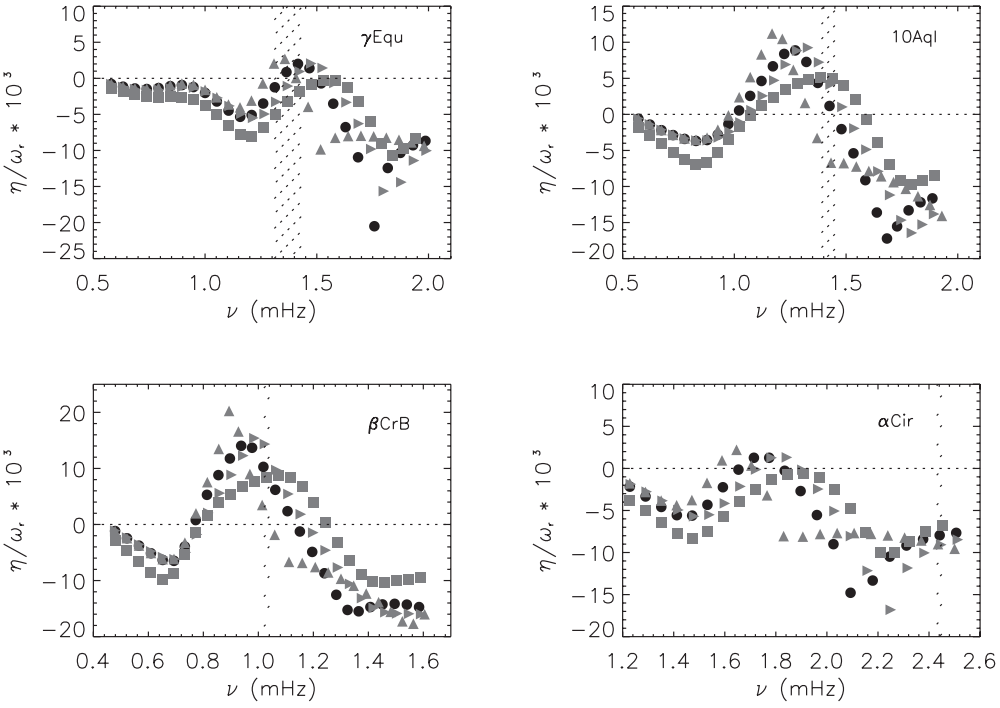

Figure 2. Normalized growth rates for polar regions (i.e. with suppression of convection in the envelope). Each panel shows the results for a different star. In addition to the three models described in Fig. 1, a fourth model is considered, with $Y_{\rm surf} = 0.1$ (right-facing triangles). The other symbols are used as in Fig. 1, but filled.

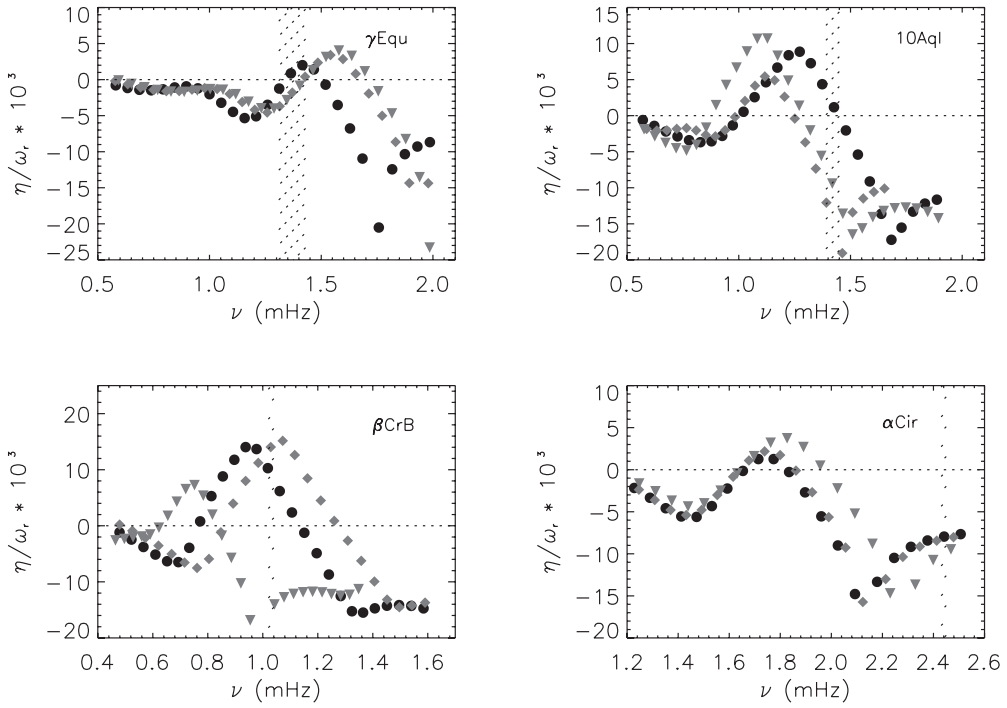

Figure 3. Comparison of normalized growth rates in polar regions for different model inputs. Each panel shows, for the star under consideration, the results for the default polar models computed with the interferometric input parameters (circles), the spectroscopic input parameters (diamonds) and the photometric input parameters (downward triangles).

pressure is responsible for the stabilization of the high radial order modes, as found by Balmforth et al. (2001) in their models. From Fig. 1, it also follows that except for the highest radial orders (above $n = 25$ for 10 Aql and β CrB, and above $n = 30$ for γ Equ and α Cir), the growth rates are almost independent of the minimum optical depth adopted in the equilibrium model, as well as of the outer boundary condition applied in the pulsation code.

3.2 Polar models

The growth rates obtained for polar models of the four stars in our sample are shown in Fig. 2. For each star, results are shown for the same three models and the same ranges of the radial orders mentioned above. One additional model, with surface helium abundance $Y_{\rm surf} = 0.1$ is also considered.

The growth rates for polar models show a distinct envelope of positive values located somewhere between radial orders 18 and 28. That envelope is more prominent in the hotter, more luminous targets, 10 Aql and β CrB, than in the cooler, less luminous targets, γ Equ and α Cir. In fact, for the latter two stars, no positive growth rates are found in this range of radial orders for models with the higher value of $\tau_{\rm min}$. It is also evident from this figure that the growth rates in polar models depend significantly on the adopted $\tau_{\rm min}$ and $Y_{\rm surf}$ as well as on the outer boundary condition applied in the pulsation code, even at moderate values of the radial order.

The theoretical description for the driving of roAp pulsations under discussion in this work suggests that the high radial order oscillations are excited in the polar regions, where convection is suppressed. Thus, we have computed, for comparison, default polar models also for the spectroscopic and photometric input parameters. The comparison between default models with the different inputs is shown in Fig. 3. For the new models, with photometric and spectroscopic inputs, we have displayed in the plots, the radial orders overlapping the frequency range adopted for the model with the interferometric inputs (which do not, in general, coincide with the radial orders displayed for the latter). Clearly, both the frequency position of the envelope of positive growth rates and the magnitude of the growth rates are significantly affected by the inputs. In particular, it is seen that the position in frequency of the envelope, for these models of similar mass, reflects essentially the dependence on the stellar radii through the scaling with $1/R^{3/2}$.

3.3 Composite models and comparison with observations

To decide on whether a given mode is excited, we need to consider the growth rates, $\eta^{\rm c}$, in the composite model composed of polar and equatorial regions matched in the way described in Section 2.2. Adopting a spherical coordinate system (r, θ, ϕ) and using $\mu = \cos\theta$, these can be obtained from the expression (Balmforth et al. 2001)

$$\eta^{\rm c}_{nlm} \approx \eta^{\rm p}_{n0} \int_{\tilde{\mu}}^{1} \left(Y^m_l\right)^2 {\rm d}\mu\, {\rm d}\phi + \eta^{\rm eq}_{n0} \int_{0}^{\tilde{\mu}} \left(Y^m_l\right)^2 {\rm d}\mu\, {\rm d}\phi$$

$$= \left(1 - \Lambda^m_l\right) \left(\frac{\Lambda^m_l}{1 - \Lambda^m_l} \eta^{\rm p}_{n0} + \eta^{\rm eq}_{n0} \right). \quad (1)$$

In the above, $\eta^{\rm p}_{n0}$ is the growth rate for the radial mode of radial order n in the polar model and $\eta^{\rm eq}_{n0}$ is the growth rate for the same mode in the corresponding equatorial model, while Y^m_l are spherical harmonic functions, with l and m representing the mode degree and azimuthal order, respectively. Moreover, the geometrical factor Λ^m_l that accounts for the extent of the polar region (hereafter the spot) is given by

$$\Lambda^m_l = (2l+1)\, \frac{(l-m)!}{(l+m)!} \int_{\tilde{\mu}}^{1} \left(P^m_l\right)^2 {\rm d}\mu,$$

where $\tilde{\mu} = \cos\vartheta$ and ϑ is the angular size of the region, centred on the magnetic pole, in which convection is assumed to be suppressed. We note that equation (1) assumes that the growth rates of non-radial modes can be estimated from those of radial modes. As argued by Balmforth et al. (2001) that assumption is justified for low-degree, high radial order modes by the fact that the driving takes place in the outer layers of the star.

From equation (1), we see that a mode is unstable in the composite model if $[\Lambda_l^m/(1-\Lambda_l^m)]\eta_{n0}^{\rm p} > -\eta_{n0}^{\rm eq}$. An illustration of the factor $\Lambda_l^m/(1-\Lambda_l^m)$ for modes of degree up to $l=2$ is presented in fig. 4 of Balmforth et al. (2001). With this criterion in mind, next we inspect the growth rates in the equatorial and polar models for each star in our sample and compare the results with the observations.

In the cases of 10 Aql and β CrB, the envelope of frequencies excited in the polar models quite clearly contains the range of observed frequencies, almost independently of the conditions assumed for $\tau_{\rm min}$ and $Y_{\rm surf}$. The match is not as good when the outer pulsation boundary condition is changed. Nevertheless, we must stress that no attempt has been made in this work to improve the match of the observations with the model results, by changing, e.g. the input parameters $T_{\rm eff}$, L within their uncertainties or by changing the stellar mass and internal chemical abundances. It is quite reasonable to assume from the frequency–radius scaling discussed in Section 3.2 that had such a search within the input parameter space been performed, good matches of the location of observed and model unstable frequencies would have been found for these two stars also when changing the outer boundary condition. Moreover, a similar exploitation of the input parameter space could easily lead to results in which the observed frequencies in these two stars are centred at the frequency of maximum polar growth rate.

From inspection of the growth rates in the equatorial models for 10 Aql, we see that their absolute value in the frequency region of interest is comparable to the maximum of the growth rates in the excitation envelops for this star ($\eta/\omega_r \sim 5$–10×10^3) in the same frequency region. Taking into consideration the term $\Lambda_l^m/(1-\Lambda_l^m)$ (cf. fig. 4 of Balmforth et al. 2001), we may then expect that excitation will take place in these models in a frequency region similar to that where modes are observed if the angular extent of the spot where convection is suppressed, ϑ, is greater than $\sim 30^\circ$. We find from the same reference that modes of $l=1$ and 2, and $m=0$ are most easily excited for spots of this size, while excitation of modes of $l=0$ requires, in this case, $\vartheta > 60^\circ$.

In the case of β CrB, inspection of the growth rates in the equatorial models shows that their absolute value in the frequency region of interest is significantly smaller than the growth rates found in polar models for the same star and frequency region. The ratio between the latter and the former is about 5. Evaluation of the term $\Lambda_l^m/(1-\Lambda_l^m)$ then leads us to conclude that axisymmetric modes of $l=1$ and 2 may be excited in the frequency region of interest for ϑ greater than about 20°, while radial modes start being excited if the spot extends more than about 35° in colatitude.

We now turn to the case of γ Equ. Keeping in mind the possibility of adjusting slightly the input parameters within their observational uncertainties to improve the match between model results and observations, as discussed above, we may conclude that mode excitation is expected in the frequency region of interest in all polar models of γ Equ considered in this work, except for that with a larger value of $\tau_{\rm min}$. Nevertheless, when comparing results in the polar and equatorial models of γ Equ, a very different picture from that seen in the cases of 10 Aql and β CrB emerges. In the present case, the absolute values of the growth rates in the equatorial models are about five times greater, or more, than the growth rates in the polar models. Therefore, excitation in the composite model requires that envelope convection is suppressed at nearly all latitudes, except for the case of $l=1$, $m=0$ modes, which become unstable if ϑ is greater than about 60°. The suppression of envelope convection in a rather large angular region could be a consequence of the intensity of the magnetic field present in γ Equ, whose mean field modulus was estimated to be $B \sim 4.0$ kG (Ryabchikova et al. 1997). However, there is little knowledge about the extent to which a magnetic field can suppress convection once it becomes nearly horizontal, as would happen in the case of a dipolar magnetic field close to the magnetic equator (Gough & Tayler 1966; Moss & Tayler 1969). Hence, the conjecture that suppression of convection may extend to such large colatitudes goes without proof.

Finally, we consider the case of α Cir. Unlike the other targets, the observations of this star raise a clear problem to the driving model discussed in this work. Inspection of the envelope of positive growth rates in polar models of α Cir would lead us to the conclusion that, if high-frequency oscillations were to be excited in this star, their frequencies should be around 1.7 mHz, rather than around 2.4 mHz, where they are observed. We note, however, that it is not the high value of the frequencies of the oscillations by itself that prevents the agreement of the model with the observations. In fact, according to fig. 4 of Cunha (2002), polar models can predict unstable modes with frequencies as high as 3.2 mHz, in stellar models of relatively low luminosity and close to the zero-age main sequence. Thus, it is the combination of high-frequency oscillations and relatively large stellar radius (of ~ 1.97 $R_\odot$) that makes it impossible for model results to agree with the observations in the case of α Cir.

4 DISCUSSION

The results presented in the preceding section highlight the importance of having access to accurate determinations of global parameters of stellar pulsators in order to test theoretical models such as the non-adiabatic models discussed here. In the case of roAp stars, that is even more evident, because their chemical peculiar nature makes the determination of the effective temperature particularly complex. Considering the four roAp stars for which angular diameters determined based on interferometric data are currently available, we were able to verify that for three of them the frequency region in which modes are predicted to be unstable, according to the models described in Balmforth et al. (2001) and Cunha (2002), agrees well with the region where frequencies are observed. Based on the comparison of model results and observations, we were also able to put constraints on the minimum extent of the angular region in which envelope convection must be suppressed, according to the proposed models.

On the other hand, we found that the fourth star in our sample, namely α Cir, represents a challenge to the excitation models proposed by Balmforth et al. (2001). One aspect of potential importance in this study is how the acoustic cutoff frequency in the models compares with the observed frequencies. As discussed in Section 2.2, one of the caveats of the models considered here is that they do not account for the direct effect of the magnetic field on pulsations. Oscillations with frequency above the acoustic cutoff are particularly sensitive to the real dynamics of the atmospheric layers of the star, where the magnetic field plays an important role. Because they neglect that effect, our models become particularly inadequate to study these high-frequency oscillations. Inspection of the default models for the four stars in our sample leads us to the

following values for their acoustic cutoff frequencies: $\nu_c \sim 1.6$ mHz for γ Equ; $\nu_c \sim 1.5$ mHz for 10 Aql; $\nu_c \sim 1.1$ mHz for β CrB; and $\nu_c \sim 1.9$ mHz for α Cir. Clearly, in the first three stars, the observed oscillations are below (albeit close to) the critical cutoff frequency, while in the case of α Cir they are well above the latter. This could be part of the reason for our lack of success with α Cir models. However, the fact that the frequency range of excitation scales with the radius of the model in a well-defined manner, together with the fact that the observed frequencies in this star are not placed where the scaling would predict, must lead us to the conclusion that an intrinsic difference exists between the case of α Cir and the case of the other three stars.

Among the roAp stars discovered so far, we could find another 11 cases, in addition to α Cir, that oscillate above ∼2 mHz. Unfortunately, a fraction of these do not have a precise parallax determination, and among those that do, only two have radii estimated based on advanced atmospheric models, such as those used in the derivation of the spectroscopic inputs considered in this work. Hence, only for these two targets, a reasonable test of agreement between model predictions and observations may be attempted (we remind the reader that polar models predict unstable oscillations as high as 3.2 mHz; thus, the fact that frequencies are above 2 mHz, by itself, does not constitute a problem to the theory). These stars are HD 24712 (HR 1217), which pulsates in the frequency range ∼2.6–2.8 mHz (Kurtz et al. 2005), and HD 137949 (33 Lib), with pulsations in the range ∼1.8–2.0 mHz (Sachkov et al. 2011). Their radii, as derived from advanced atmospheric models, are, respectively, $R = 1.778$ $R_\odot$ for HD 24712 (Shulyak et al. 2009) and $R = 2.13$ $R_\odot$ for HD 137949 (Shulyak et al. 2013).

Accepting the global parameters derived by Shulyak et al. (2009, 2013), we find that HD 24712 is slightly beyond the red edge of the instability strip derived by Cunha (2002), meaning that in default polar models of this star, no high frequencies are expected to be found unstable. If we ignore this fact for a moment and consider the scaling with radius of the envelop of growth rates (ignoring the small mass dependence expected in that scaling), we find, in addition, that the envelope would be centred around 2.0 mHz, for the radius considered, thus significantly out of place in relation to the observed frequencies. For these two reasons, it is reasonable to accept that HD 24712 is an example of the group of roAp stars whose pulsations cannot be explained by the excitation in models with convection suppressed. On the other hand, HD 137949 is located well within the instability strip predicted by default polar models, but if we consider the same scaling, we find that its radius would have to be ∼1.8 $R_\odot$ in order for its pulsations to be explained by the models under discussion. So, either this star is significantly hotter than that predicted by Shulyak et al. (2013), with an effective temperature around 8000 K, or, more likely, it is another example of the same group.

In summary, if we extend our sample to include also HD 24712 and HD 137949, for which there are no interferometric data, but there are radii determinations based on advanced stellar models that account for element stratification, we find that in the new sample of six stars, half exhibit oscillations in the frequency region predicted by the models with convection suppressed, which is close, but below the acoustic cutoff frequency of the models, while in the other half, the observed oscillations are significantly above the predicted region. Thus, there is a group of roAp stars, namely that in which observed pulsation frequencies are clearly above the critical cutoff frequency expected for their position in the HR diagram, for which the driving of the oscillations cannot currently be explained by the models proposed by Balmforth et al. (2001). We should add that this conclusion can hardly be changed by varying the inputs to the equilibrium model, such as the interior metallicity or helium abundance. The reason is that such changes, while keeping the radius fixed, will impact on the results mostly through a small change in the mass of the model, which will hardly influence the position of the envelope of excited modes. Given that the driving in the alternative non-adiabatic models proposed in the literature (Gautschy et al. 1998; Saio 2005; Théado et al. 2009) originates also on the opacity mechanism working on the hydrogen ionization region, we expect that similar difficulties would be found when attempting to use these models to explain the observations (and in fact, such was confirmed by Saio in a private communication).

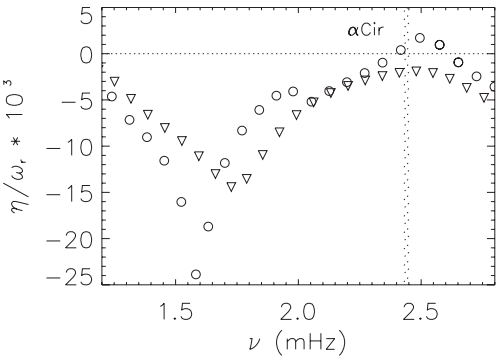

Figure 4. Normalized growth rates in equatorial models with different atmospheric properties. Both models were computed with photometric inputs. The open circles show results for a model similar to the default equatorial model, but with helium settling and $Y_{\rm surf} = 0.08$. The open triangles are for a model with a solar-like atmosphere in which the $T-\tau$ relation is derived from a model C of Vernazza et al. (1981) adopting $\tau_{\rm min} = 10^{-4}$.

It is worth noting that while studying equatorial models for α Cir with different atmospheres or with He diffusion, we succeeded in finding cases in which modes similar to those observed in this star are excited or in which their growth rates, while still negative, approach zero. An example of the results for such models, namely a model with a solar-like atmosphere in which the $T-\tau$ relation is derived from a model C of Vernazza, Avrett & Loeser (1981) and a model similar to the default equatorial model, but with helium settling and $Y_{\rm surf} = 0.08$, is shown in Fig. 4. Inspection of the work integrals shows that in these cases, the strongest contribution for the mode energy input still comes from the region of hydrogen ionization, but in this case, the driving agent is the turbulent pressure, rather than the opacity. In fact, a similar driving effect of the turbulent pressure has been seen also in δ-Scuti stars by Antoci et al. (in preparation) for intermediate radial order modes. Unfortunately, since our models do not retain the complete dynamics experienced by these very high frequency oscillations in the atmospheric layers, we refrain from further exploring this potential solution for the driving of the oscillations in stars like α Cir. Nevertheless, these results indicate that excitation of modes with frequencies above the acoustic cutoff in the hydrogen ionization region is not impossible in models with convection.

ACKNOWLEDGEMENTS

MSC is supported by an Investigador FCT contract funded by FCT/MCTES (Portugal) and POPH/FSE (EC). IMB acknowledges financial support from the FCT (Portugal) through the SFRH/BPD/87857/2012. This research made use of funds from

the ERC, under FP7/EC, through the project FP7-SPACE-2012-312844. Part of this research was funded through an International Research Collaboration Award of the University of Sydney.

REFERENCES

Alentiev D., Kochukhov O., Ryabchikova T., Cunha M., Tsymbal V., Weiss W., 2012, MNRAS, 421, L82
Asplund M., Grevesse N., Sauval A. J., Scott P., 2009, ARA&A, 47, 481
Balmforth N. J., 1992, MNRAS, 255, 603
Balmforth N. J., Cunha M. S., Dolez N., Gough D. O., Vauclair S., 2001, MNRAS, 323, 362
Balona L. A. et al., 2011a, MNRAS, 410, 517
Balona L. A. et al., 2011b, MNRAS, 413, 2651
Bruntt H. et al., 2008, MNRAS, 386, 2039
Bruntt H. et al., 2009, MNRAS, 396, 1189
Bruntt H. et al., 2010, A&A, 512, A55
Cunha M. S., 2002, MNRAS, 333, 47
Cunha M. S., 2007, Commun. Asteroseismol., 150, 48
Cunha M. S. et al., 2007, A&AR, 14, 217
Elkin V. G., Riley J. D., Cunha M. S., Kurtz D. W., Mathys G., 2005, MNRAS, 358, 665
Gautschy A., Saio H., Harzenmoser H., 1998, MNRAS, 301, 31
Gough D. O., 1977, in Spiegel E. A., Zahn J.-P., eds, Lecture Notes in Physics, Vol. 71, Problems of Stellar Convection. Springer-Verlag, Berlin, p. 349
Gough D. O., Tayler R. J., 1966, MNRAS, 133, 85
Grevesse N., Noels A., 1993, in Prantzos N., Vangioni-Flam E., Casse M., eds, Origin and Evolution of the Elements. Cambridge Univ. Press, Cambridge, p. 15
Gruberbauer M. et al., 2008, A&A, 480, 223
Hatzes A. P., Mkrtichian D. E., 2004, MNRAS, 351, 663
Huber D. et al., 2008, A&A, 483, 239
Hubrig S. et al., 2005, A&A, 440, L37
Kochukhov O., 2009, Commun. Asteroseismol., 159, 61
Kochukhov O., Bagnulo S., 2006, A&A, 450, 763
Kochukhov O., Shulyak D., Ryabchikova T., 2009, A&A, 499, 851
Kreidl T. J., Kurtz D. W., 1986, MNRAS, 220, 313
Kurtz D. W., 1982, MNRAS, 200, 807
Kurtz D. W. et al., 2005, MNRAS, 358, 651
Kurtz D. W., Elkin V. G., Mathys G., 2007, MNRAS, 380, 741
Kurtz D. W. et al., 2011, MNRAS, 414, 2550
Moss D. L., Tayler R. J., 1969, MNRAS, 145, 217
Nesvacil N., Shulyak D., Ryabchikova T. A., Kochukhov O., Akberov A., Weiss W., 2013, A&A, 552, A28
Perraut K. et al., 2011, A&A, 526, A89
Perraut K. et al., 2013, A&A, preprint (arXiv:1309.4423)
Ryabchikova T. A., Adelman S. J., Weiss W. W., Kuschnig R., 1997, A&A, 322, 234
Sachkov M., Hareter M., Ryabchikova T., Wade G., Kochukhov O., Shulyak D., Weiss W. W., 2011, MNRAS, 416, 2669
Saio H., 2005, MNRAS, 360, 1022
Saio H., Gruberbauer M., Weiss W. W., Matthews J. M., Ryabchikova T., 2012, MNRAS, 420, 283
Serenelli A. M., Basu S., 2010, ApJ, 719, 865
Shibahashi H., Saio H., 1985, PASJ, 37, 245
Shulyak D., Tsymbal V., Ryabchikova T., Stütz C., Weiss W. W., 2004, A&A, 428, 993
Shulyak D., Ryabchikova T., Mashonkina L., Kochukhov O., 2009, A&A, 499, 879
Shulyak D., Ryabchikova T., Kochukhov O., 2013, A&A, 551, A14
Sousa S. G., Cunha M. S., 2008, MNRAS, 386, 531
Théado S., Vauclair S., Cunha M. S., 2005, A&A, 443, 627
Théado S., Dupret M.-A., Noels A., Ferguson J. W., 2009, A&A, 493, 159
Vernazza J. E., Avrett E. H., Loeser R., 1981, ApJS, 45, 635

This paper has been typeset from a TEX/LATEX file prepared by the author.